Supporting Information

Shim et al. 10.1073/pnas.1205309109

SI Experimental Procedures

Cell Culture, Construct Design, and BacMam Virus Generation. Sf9 cells were maintained in suspension on orbital shakers in a 27 °C room in TNM-FH medium supplemented with 8% (vol/vol) heat-inactivated FBS. *N*-acetylglucosaminyltransferase I (GnTI$^-$) HEK293 cells (1) were maintained in the CDM4HEK medium, (HyClone) supplemented with 4% (vol/vol) FBS, on orbital shakers in a 37° C water-jacketed incubator with 5% (vol/vol) CO_2. The coding sequences of human M-CSF receptor-binding domain (residues 4–150 of the mature peptide: SEYCSHMIGSGHLQSLQRLIDSQMETSCQITFEFVDQEQLKDPVCYLKKAFLLVQDIMEDTMRFRDNTPNAIAIVQLQELSLRLKSCFTKDYEEHDKACVRTFYETPLQLLEKVKNVFETKNLLDKDWNIFSKNCNNSFAECSSQD) and the cDNA fragment encoding EBV BARF1 (residues 18–221: QAVTAFLGERVT LTSYWRRVSLGPEIEVSWFKLGPGEEQVLIGRMHHDVIFIEWPFRGFFDIHRSANTFFLVVTAANISHDGNYLCRMKLGETEVTKQEHLSVVKPLTLSVHSERSQFPDFSVLTVTCTVNAFPHPHVQWLMPEGVEPAPTAANGGVMKEKDGSLSVAVDLSLPKPWHLPVTCVGKNDKEEAHGVYVSGYLSQ), with C-terminal 6-His tag, were subcloned separately into the baculovirus-mediated mammalian cell gene transduction (BacMam) vector pVLAD6 (1). The constructs and the BacVector-3000 baculovirus DNA (EMD Chemicals) were used to cotransfect sf9 cells in six-well plates in the presence of Insect GeneJuice transfection reagent (EMD Chemicals). After the transfected cells were incubated at 27° for 5 d, each of the resulting low-titer virus stocks was harvested and was used to infect ~2 L of Sf9 cells at 2×10^6 cells/mL for amplification. The amplified viruses were harvested when >50% of the infected sf9 cells were lysed.

Protein Expression and Purification. The amplified BARF1 and macrophage colony-stimulating factor (M-CSF) BacMam viruses were used to infect 4 L of HEK293 GnTI$^-$ cells individually at a density of 1.5×10^6 cells/mL After 72 h, the cells were pelleted with low-speed centrifugation ($600 \times g$), and the supernatants were collected and concentrated to less than 500 mL. The recombinant proteins in the supernatant were captured by Talon metal affinity resin (Clontech) in batches and were eluted with 250 mM imidazole, pH7.5. The eluted BARF1 and M-CSF proteins were glycan-minimized with endoglycosidase F1 (Sigma), leaving one *N*-acetylglucosamine residue at each Asn-linked glycosylation site after digestion, and were treated with bovine carboxypeptidase A to remove C-terminal His-tags. The trimmed products were combined at an appropriate ratio with a slight excess of M-CSF and were purified further with gel filtration columns (Superdex-200; Amersham Biosciences) in Hepes-buffered saline (HBS) buffer [10 mM Hepes (pH7.5), 150 mM NaCl]. The fractions corresponding to the stoichiometric BARF1:M-CSF complex were pooled together and were concentrated with a Vivaspin centrifugal device (Vivascience) ($1{,}000 \times g$) to 14 mg/mL.

Crystallization. Vapor diffusion crystallization in the sitting-drop format was performed at room temperature. The drops contained equal volumes (0.5 μL) of reservoir solution and protein solution and were equilibrated against the reservoir solution [8% PEG8000, 0.1 M imidazole (pH 8.0), 0.22M calcium acetate] in a 20° incubator.

X-Ray Data Collection. Crystals were transferred gradually from the reservoir solution to a cryo-protecting solution [8% PEG8000, 0.1 M imidazole (pH8.0), 0.22 M calcium acetate, 25% ethylene glycol] and were flash-cooled in liquid nitrogen in crystal-mounting loops. X-ray diffraction was performed at the LS-CAT beamline 21-ID-G of Advanced Photon Source (Argonne, IL). The data were indexed, integrated, and scaled with HKL2000 (2). The data-processing statistics are summarized in Table S1.

Structure Determination and Refinement. Three copies of BARF1 in the asymmetric unit were located by molecular replacement using the program PHASER (3), with the free BARF1 structure (PDB ID code 2CH8) (4) as the search model. The partial structure was used to generate initial model phases, which subsequently were improved by threefold noncrystallographic symmetry averaging as implemented during the process of solvent flattening and density modification. The improved phases were used to generate a Fourier synthesis electron density map in which the four-helix bundle-shaped electron densities for M-CSF were clearly discernible. The mouse M-CSF (PDB ID code 3EJJ) model then was placed manually into the unoccupied densities, and the sequence was corrected to human M-CSF. The complex model was rebuilt using COOT (5) and was refined with the Refmac program (6). Water molecules were added automatically with COOT and validated with electron density maps. The refinement statistics are summarized in Table S1.

Isothermal Titration Calorimetry. Calorimetric titrations were implemented with a VP-ITC calorimeter (MicroCal) at 30 °C. Using gel filtration chromatography (Superdex-200, Amersham Biosciences), all proteins to be used in the titrations were buffer-exchanged into an identical lot of HBS buffer [10 mM Hepes (pH7.5), 150 mM NaCl] to minimize the dilution effects of buffer heat during titration. The protein samples were degassed for 5 min before being loaded separately into the reaction chamber and injection syringe. In the BARF1:M-CSF–binding experiments, human M-CSF was loaded into the syringe as injectant. In the tyrosine kinase colony-stimulating factor receptor (FMS)–binding experiments, human M-CSF or the BARF1:M-CSF complex was loaded into the syringe as injectant. The proteins in the syringe were injected into the reaction chamber in 3-μL pulses at 5-min intervals. The data were processed with MicroCal Origin 5.0 software.

Phosphorylation Assay. COS7 or HEK293H cells were infected with full-length human or mouse FMS BacMam virus for 6 h and then were serum starved overnight and stimulated with 75 nM M-CSF or 75 nM BARF1:M-CSF for 2 min (COS-7 cells) or with a range of concentrations (6.25–75 nM) (HEK293H cells). The stimulated cells were washed with cold PBS and lysed with Triton-X lysis buffer. The lysates were spun down, and the supernatant was collected. Equal amounts of the samples were run on an SDS/PAGE gel, transferred to PVDF membranes, and immunoblotted with anti–M-CSF receptor and anti–phospho-M-CSF receptor (Tyr723) (Cell Signaling Technology). The blots were developed using the WesternBreeze Immunodetection Kit (Invitrogen). Alternatively, membranes were incubated with an HRP-conjugated goat anti-rabbit secondary antibody (Cell Signaling Technology) and visualized by ECL (Amersham). Band intensities were quantified using ImageJ 1.45p software. Because of the large variation in quantifying faint bands, the difference between negative control and the residual phosphorylation of the BARF1:M-CSF complex does not appear statistically significant. However, the residual, above-background signaling of

the complex was observed consistently using both human FMS and mouse FMS and in both COS7 cells and HEK293H cells, as shown in Fig. 1 and Fig. S3. The receptors were expressed at higher levels in HEK293H cells than in COS7 cells, allowing easier visualization of the reduced phosphorylation induced by the BARF1:M-CSF complex but at the same time narrowing the difference between M-CSF induction and BARF1:M-CSF induction.

1. Dukkipati A, Park HH, Waghray D, Fischer S, Garcia KC (2008) BacMam system for high-level expression of recombinant soluble and membrane glycoproteins for structural studies. *Protein Expr Purif* 62:160–170.
2. Otwinowski Z, Minor W (1997) Processing of X-ray diffraction data collected in oscillation mode. *Methods Enzymol* 276:307–326.
3. McCoy AJ, et al. (2007) Phaser crystallographic software. *J Appl Cryst* 40:658–674.
4. Tarbouriech N, Ruggiero F, de Turenne-Tessier M, Ooka T, Burmeister WP (2006) Structure of the Epstein-Barr virus oncogene BARF1. *J Mol Biol* 359:667–678.
5. Emsley P, Cowtan K (2004) Coot: Model-building tools for molecular graphics. *Acta Crystallogr D Biol Crystallogr* 60:2126–2132.
6. Murshudov GN, Vagin AA, Dodson EJ (1997) Refinement of macromolecular structures by the maximum-likelihood method. *Acta Crystallogr D Biol Crystallogr* 53:240–255.

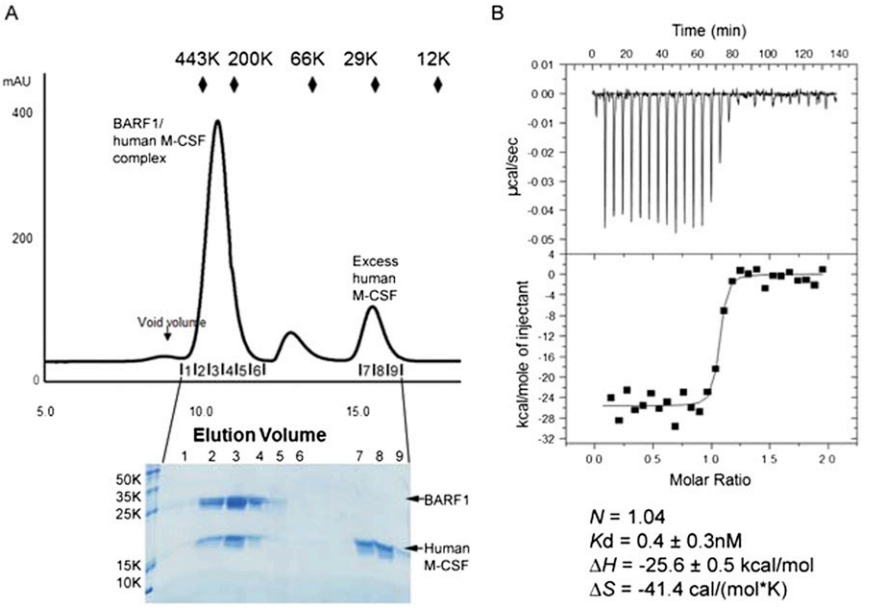

Fig. S1. BARF1 and M-CSF form a high-affinity, stable complex. (*A*) Gel filtration analysis of the coexpressed BARF1:human M-CSF complex in calibrated Superdex-200 chromatography. SDS/PAGE of the fractions is shown below. (*B*) Isothermal titration calorimetry analysis of the binding between BARF-1 and human M-CSF. The overall stoichiometry, affinity, enthalpy, and entropy changes of the reaction are shown below. The molar ratio of ~1 is consistent with one BARF1 hexamer binding to three M-CSF dimers.

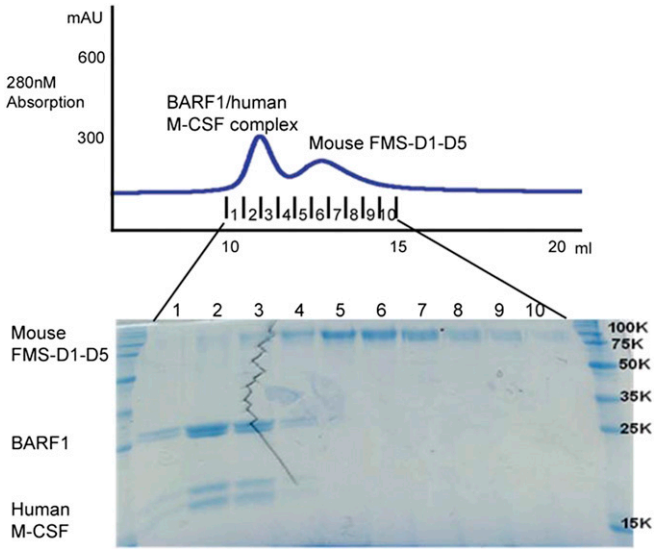

Fig. S2. BARF1, M-CSF, and FMS do not form ternary complexes in gel filtration but are a binary BARF1:M-CSF complex and FMS alone. (*Upper*) Chromatograph of the three proteins (BARF1, human M-CSF, and mouse FMS-D1-D5) combined, as resolved in the Superdex-200 column. (*Lower*) SDS/PAGE analysis of the fractions from gel filtration. Note that mouse FMS–D1–D5 is eluted as a wide peak, probably because of its five-domain, extended conformation.

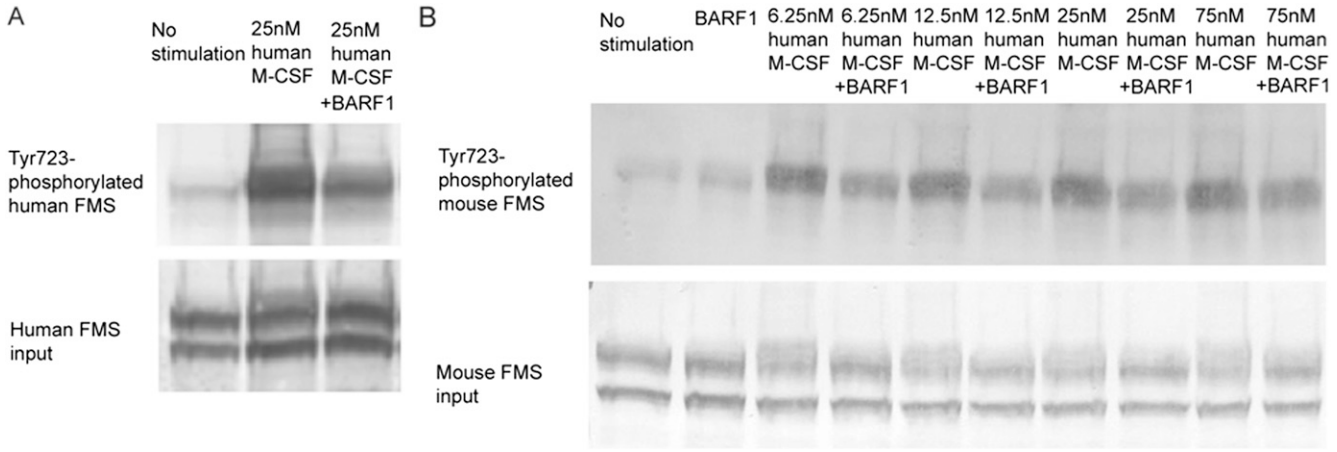

Fig. S3. BARF1 reduces ligand-induced FMS phosphorylation. (*A*) HEK293H cells expressing human FMS were stimulated with 25 nM human M-CSF or the human M-CSF:BARF1 complex for 2 min. (*B*) HEK293H cells expressing mouse FMS were stimulated with 6.25–75 nM human M-CSF or the human M-CSF:BARF1 complex for 2 min. Western blot analysis was used to detect total and Tyr723-phosphorylated FMS of cell lysates. In all the different stimulant concentrations, the lanes treated with M-CSF alone showed higher phosphorylation levels than the lanes treated with BARF1:M-CSF; however, BARF1:M-CSF–stimulated phosphorylation levels were above background level.

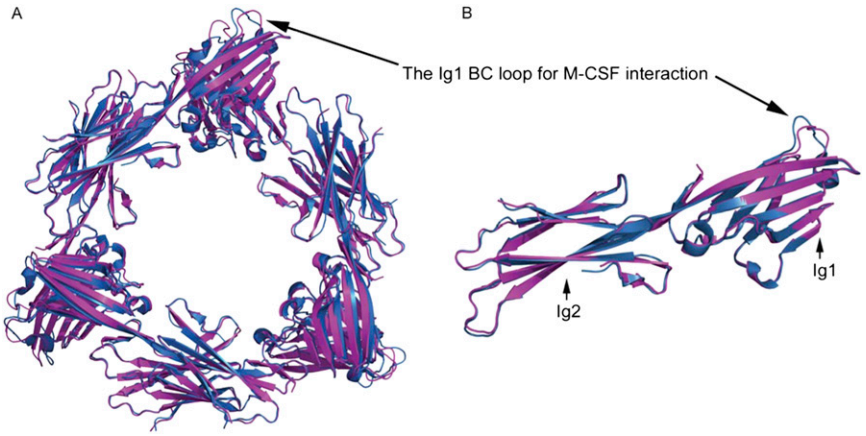

Fig. S4. Comparison between the free BARF1 (PDB ID code 2CH8) and the M-CSF–bound BARF1. (*A*) Superimposition of the entire hexameric BARF1 rings in free (blue) and M-CSF–bound (magenta) states. (*B*) Superimposition of a BARF1 protomer in free and bound states. Note that the hexameric BARF1 structure is highly inelastic because of the ring restraints. The only significant difference between free *BARF1* and enthalpy in complex with M-CSF is at the Ig domain 1 (Ig1) loops that are used in M-CSF binding.

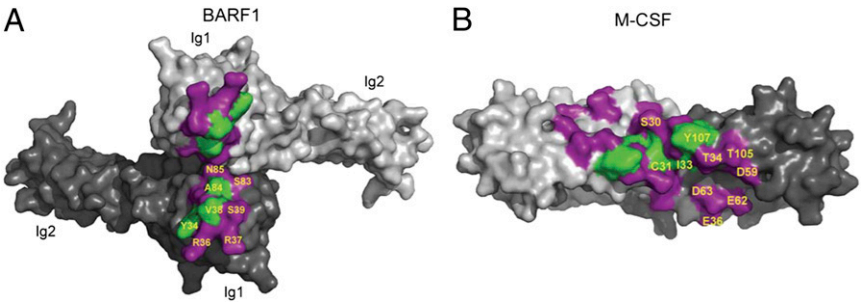

Fig. S5. The BARF1:M-CSF binding surfaces. (*A*) The M-CSF–binding surface of BARF1. (*B*) The BARF1-binding surface of human M-CSF. The noninterface residues for the different protomers in the dimers are shown in gray and silver. The interface is colored green for hydrophobic residues and magenta for hydrophilic residues.

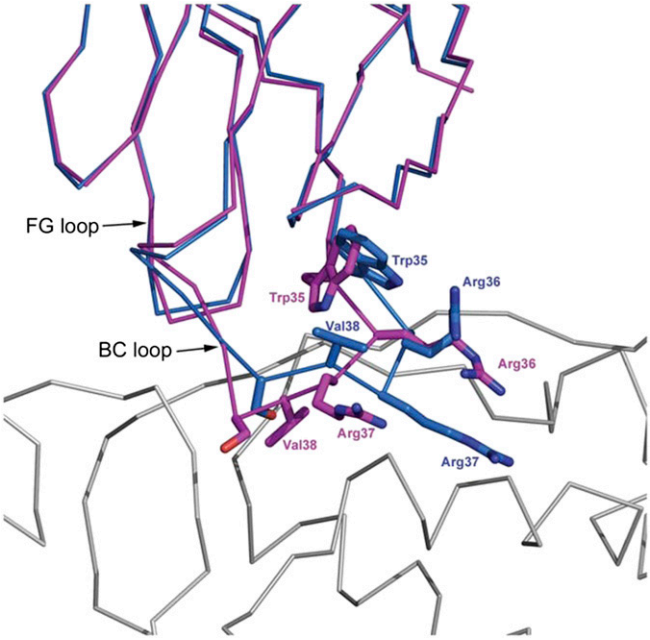

Fig. S6. The rearrangement of the BARF1 Ig1 BC loop for M-CSF binding. Free BARF1 is colored cyan, and the M-CSF–bound BARF1 is colored magenta. The bound human M-CSF is shown as gray traces for reference.

Table S1. Data collection and refinement statistics

Data collection	
Space group	C2
Cell dimensions (Å)	
a	199.55
b	162.70
c	57.34
α,β,γ (°)	90, 95.87, 90
Wavelength (Å)	0.9786
Resolution range (Å)(highest resolution shell)	20–2.2 (2.3–2.2)
Unique reflections	89831
Completeness (%)	97.2 (90.5)
I/σ (I)	17.85 (3.6)
Redundancy	3.3
R_{merge} (%)*	8.1 (27.0)
Refinement	
Resolution range (Å)(highest resolution shell)	20–2.2 (2.3–2.2)
R_{cryst}†	0.222
R_{free}†	0.266
No. atoms (average B-factors)	
Protein	
Carbohydrate	
Water	
Rmsd bond length (Å)	0.01
Rmsd bond angle (°)	1.3
Ramachandran (favored, allowed, generally allowed, disallowed) (%)	91.6, 8.2, 0.2, 0

*$R_{merge} = \sum_{hkl}|I-\langle I\rangle|/\sum_{hkl}I$, where I is the intensity of unique reflection hkl, and $\langle I\rangle$ is the average over symmetry-related observation of unique reflection hkl.

†$R_{cryst} = \sum|F_{obs}-F_{calc}|/\sum F_{obs}$, where F_{obs} and F_{calc} are the observed and the calculated structure factors, respectively. R_{free} is calculated using 5% of reflections sequestered before refinement.

Table S2. Salt bridges between each BARF1 protomer and two M-CSF monomers at each half interface

BARF1	M-CSF (helix αB and strand β1-contributing protomer)
Arg36	Glu36
Arg36	Asp59
Arg36	Asp63
Arg37	Asp63

Table S3. Hydrogen bonds between each BARF1 protomer and two M-CSF monomers at each half interface

BARF1	Atom	M-CSF (helix αB and strand β1-contributing protomer)	Atom	M-CSF (loop αA-β1–contributing protomer)	Atom	Distance (Å)
Arg36	Nη2	Asp59	O			2.7
Val38	N	Asp63	O			3.0
Val38	O			Ser30	N	3.2
Leu40	O			Ser30	Oγ	2.7
Arg82	Nη1			Ser30	O	3.4
Arg82	Nη2			Gln32	Oε1	2.6
Ala84	O			Ser30	Oγ	3.2
Asn85	Oδ1	Thr34	N			3.0
Asn85	Nδ2	Thr34	O			3.0
Asn85	N			Ser30	Oγ	3.3

Table S4. Van der Waals contacts (cutoff 4 Å) between each BARF1 protomer and two M-CSF monomers at each half interface

BARF1	M-CSF (helix αB and strand β1-contributing protomer)	M-CSF (loop αA-β1–contributing protomer)
Tyr34	Thr34, Glu36, Thr105	
Arg36	Glu36, Asp59, Asp63	
Arg37	Glu62, Asp63, Arg66	
Val38	Ile33, Thr34, Asp63, Thr64	Glu28, Thr29, Ser30
Ser39	Arg66	Glu28, Thr29, Ser30
Leu40		Ser30
Gly41		Ser30
Arg82		Gln32, Ser30
Ser83	Tyr107	
Ala84	Gln32, Ile33	Ser30, Cys31
Asn85	Ile33, Thr34	Ser30
Thr86	Thr34, Tyr107	
Phe88	Tyr107	